Chinese Journal of
POLYMER SCIENCE

ARTICLE

https://doi.org/10.1007/s10118-018-2097-8
Chinese J. Polym. Sci. 2018, 36, 943–952

Mono- and Binuclear Cobalt(II) Complexes Supported by Quinoline-2-imidate Ligands: Synthesis, Characterization, and 1,3-Butadiene Polymerization

Heng Liu[a], Rui Zhuang[a,b], Bo Dong[a,c], Feng Wang[a], Yan-Ming Hu[a*], and Xue-Quan Zhang[a*]

[a] *CAS Key Laboratory of Synthetic Rubber, Changchun Institute of Applied Chemistry, Chinese Academy of Sciences, Changchun 130022, China*
[b] *University of Chinese Academy of Sciences, Beijing 100049, China*
[c] *College of Materials Science and Engineering, Jilin University, Changchun 130022, China*

Abstract A series of mono- and binuclear Co(II) complexes (**Co1**–**Co7**) supported by quinoline-2-imidate ligands were synthesized and thoroughly characterized. Measured by single crystal X-ray crystallography, complexes **Co1** and **Co3** adopted distorted tetrahedral structures around the cobalt center. Upon activation by ethylaluminium sesquichloride (EASC), these cobalt complexes exhibited high catalytic activity and *cis*-1,4-selectivity towards 1,3-butadiene polymerization. The effects of ligand environment, polymerization temperature, and cocatalyst types on the polymerization were investigated in detail. Interestingly, the binuclear Co(II) complexes exhibited high thermal stability, and the polymer yields were up to 97.2% even at a high temperature of 70 °C.

Keywords Late transition metal; Cobalt(II) complexes; Coordination polymerization; Polybutadiene

Citation: Liu, H.; Zhuang, R.; Dong, B.; Wang, F.; Hu, Y. M.; Zhang, X. Q. Mono- and Binuclear Cobalt(II) Complexes Supported by Quinoline-2-imidate Ligands: Synthesis, Characterization, and 1,3-Butadiene Polymerization. Chinese J. Polym. Sci. 2018, 36(8), 943–952.

INTRODUCTION

Imine-based late-transition metal complexes have played a pivotal role in the ethylene polymerization ever since the discovery by Brookhart in the 1990s, a seminal report on Ni(II) and Pd(II) complexes catalyzing ethylene homopolymerization and copolymerization with acrylates that has set the ground for later rapid advances in the catalysis of olefin polymerization[1−18]. Due to the inherent advantages of these late-transition metals, such as high catalytic activity, cost-effectiveness, ease of manipulation, eco-friendliness, *etc*., such kind of precursors were also used to catalyze 1,3-butadiene (BD) polymerization during the past decade. It has been surprisingly found that, besides ligand skeleton and polymerization conditions, the catalysts' performance and the properties of resulting polymers can be finely-tuned by the metal centers[19−22]. For instance, Fe(II)- and Fe(III)-based complexes are apt to produce polybutadienes (PBDs) with high *trans*-1,4 content; the resulting PBDs have a considerable degree of crystallization and experience a strain-induced crystallization and consequently are necessary for the production of high-performance tires[23, 24]. Ni(II) complexes usually produce polymers with mediate *cis*-1,4 content and low molecular weight[25], which are mostly used as adhesives, sealants, additives, *etc*. On the other hand, Co(II)-based complexes are more attention-grabbing because they possess high *cis*-1,4 stereoselectivity[26−29], producing polymers to behave much like natural rubber. In addition, Co(II)-based systems are also good candidates in preparing 1,2-PB in the presence of external donors. Till now, diversified imine-based Co(II) complexes have been designed and employed to initiate BD polymerization, including bis(imino)pyridine Co(II)[30], α-diimine Co(II)[31], β-triketimine Co(II)[32, 33], bis(salicylaldiminate) Co(II)[27, 34, 35], pyridine-2-imine Co(II)[36], (1,10-phenanthroline-2-pyrazolyl) Co(II)[37], bis(oxazolinyl) pyridine Co(II)[38], bis(imidazolyl)pyridine Co(II)[39, 40], bis(benzimidazolyl)amine Co(II)[41], *etc*. Despite of these advances, the answer to how the ligand structures affect the catalytic activity of corresponding complexes is still blurred. Some clues were given in a recent report, in which incorporating various substituents bearing different electronic and steric properties to aryl rings by employing different aniline analogues showed obvious influence on the catalytic behaviors[30]. However, changing the substitutents on other parts of imine group is still untapped yet. In our previous studies, we developed a series of imidoylchloride-based Co(II) complexes. It was excitingly found that introducing halogen atom, a electron-withdrawing group, to imine-carbon could increase the electropositivity of the metal centre and thus led to higher catalytic activity[42, 43].

---

* Corresponding authors: E-mail ymhu@ciac.ac.cn (Y.M.H.)
E-mail xqzhang@ciac.ac.cn (X.Q.Z.)

Received October 27, 2017; Accepted November 27, 2017;

However, the effect of substituents at imine-carbon position on the catalytic behaviors of BD polymerization is rarely investigated. As an extension of our previous work, we synthesized a series of imidate-based ligands with ether group at C=N carbon position by using the imidoylchloride precursors, and disclosed the catalytic behaviors of the corresponding Co(II) complexes towards BD polymerization.

Imine-based multinuclear olefin polymerization catalysts are another hot spot in recent years. The interesting catalytic properties were revealed when they were used in olefin polymerization and copolymerization[44−46]. For instance, the linked phenoxyiminato group IV complexes led to significantly greater extents of comonomer enchainment because of the close enforced contact between two catalytic centres[47]. Xanthene-bridged dinuclear α-diimine Ni complexes showed good thermal stability and high catalytic activity, generating polyethylenes with high molecular weights, narrow polydispersities and very low branching density[48]. Macrocycle trinuclear 2,6-bis(imino)pyridyl iron precatalysts exhibited much higher activity and longer lifetime for ethylene polymerization as compared to the mononuclear anolgues[49]. However, multinuclear catalysts for diene polymerization are quite limited. Only one paper reported that the tridentate NNO dinuclear Co(II) complexes were employed and performed high *cis*-1,4-selectivity and high thermal tolerance at elevated temperatures[28]. Herein, we report the preparation of a series of imidate-based binuclear Co(II) complexes by using different kinds of diols to react with imidoylchloride, and their catalytic behaviors for butadiene polymerization have been further investigated.

EXPERIMENTAL

Materials and Characterization

All manipulations of air and/or moisture sensitive compounds were carried out under a dry and oxygen-free argon atmosphere by using Schlenk techniques or under a nitrogen atmosphere in a glove box. The solvents were refluxed over CaH_2 or sodium-benzophenone and distilled prior to use. 1,3-Butadiene was obtained from Jinzhou Petrochemical Company. $CoBr_2$ and $CoCl_2$ were purchased from Alfa Aesar. Ethylaluminum sesquichloride (EASC), diethylaluminum chloride (DEAC) and methyl aluminoxane (MAO) were purchased from Akzo Noble and used as received. 1,4-Dihydroxybenzene, bisphenol A, and 4,4′-methylene diphenol were purchased from Aladdin company. 2-[*N*-(2,6-diisopropylphenyl)carboximidoyl-chloride] quinoline was synthesized according to the method described in the literature[43].

^{1}H-NMR (400 MHz) and ^{13}C-NMR (100 MHz) were recorded on a Varian Unity spectrometer in $CDCl_3$ at ambient temperature using tetramethylsilane as an internal standard. FTIR spectra were recorded on a BRUKE Vertex-70 FTIR spectrometer. Mass spectrometric detection was carried out on a Xevo TQ 151 mass spectrometer (Waters Corp., Milford, MA, USA) with a 152 electrospray ionization (ESI) source. Elemental analysis was performed on an elemental Vario EL spectrophotometer. The proportions of *cis*-1,4 and *trans*-1,4 units of polymer were determined by FTIR spectra, ^{1}H-NMR, and ^{13}C-NMR. The number-average molecular weights (M_n) and molecular weight distributions (M_w/M_n) of polymers were measured at 30 °C by gel permeation chromatography (GPC) equipped with a Waters 515 HPLC pump, four columns (HMW 7 THF, HMW 6E THF×2, HMW 2 THF), and a Waters 2414 refractive index detector. Tetrahydrofuran (THF) was used as an eluent at a flow rate of 1.0 mL/min. The values of M_n and M_w/M_n were determined by using polystyrene calibration.

Preparation and Characterization of Ligands and Complexes

*General procedures for the synthesis of ligands **L1**–**L4***

Ligands **L1**–**L4** were prepared in a similar manner using 2-[*N*-(2,6-diisopropylphenyl)carboximidoylchloride]quinoline precursor which were synthesized by a similar method according to the literature[43]. A typical synthetic procedure of the ligand **L1** is described as follows:

To a 100 mL round-bottom flask were added 20 mL of THF and 0.192 g of methanol (6 mmol) under nitrogen atmosphere, then the flask was put into an ice bath and 0.14 g of sodium (6 mmol) was carefully added into the flask (a lot of hydrogen gas bubbled out!). The mixture was stirred for 2 h at room temperature and then refluxed for 2 h. Then 2-[*N*-(2,6-diisopropylphenyl)carboximidoylchloride]quinoline (0.7 g, 2 mmol) in 20 mL of THF was added dropwise into the flask, and the solution was further refluxed for 12 h. Then 10 mL of water and 30 mL of CH_2Cl_2 were added, and the mixture was further washed with 100 mL of water for three times. The organic layer was collected and dried over anhydrous magnesium sulfate. The solvent was evaporated under reduced pressure, and then the residue was purified by column chromatography on silica with the eluent of petroleum ether:ethyl acetate (V:V = 10:1) to afford a yellow solid.

The ligand of 2-[methyl(*N*-diisopropylphenylcarboximidate)]quinoline (**L1**). Yield: 84.7%. ^{1}H-NMR (400 MHz, $CDCl_3$, δ, ppm): 8.00 (d, 1H, $H_{quinoline\text{-}4}$), 7.96 (d, 1H, $H_{quinoline\text{-}8}$), 7.71 (d, 1H, $H_{quinoline\text{-}3}$), 7.66 (t, 1H, $H_{quinoline\text{-}5}$), 7.51 (t, 1H, $H_{quinoline\text{-}7}$), 7.27 (partially overlapping with $CDCl_3$, ppm), 6.95–7.01 (m, 3H, H_{Ar}), 4.14 (s, 3H, $-OCH_3$), 3.03 (m, 2H, $-CH^*(CH_3)_2$), 1.23 (d, 6H, $-CH_3$), 0.87 (d, 6H, $-CH_3$). ^{13}C-NMR (100 MHz, $CDCl_3$, δ, ppm): 154.75, 149.7, 147.4, 143.2, 142.8, 137.2, 135.9, 130.1, 129.7, 127.6, 127.3, 122.9, 122.8, 120.3, 54.5, 28.2, 23.6, 22.4. FTIR (KBr, cm^{-1}): 3062(w), 2964(m), 2867(m), 1679(s), 1588(m), 1499(m), 1463(m), 1424(m), 1380(m), 1341(m), 1280(m), 1242(m), 1212(m), 1150(m), 1095(m), 997(m), 900(m), 838(m), 793(m), 751(m), 727(m). Anal. Calcd. for $C_{23}H_{26}N_2O$ (346.2): C, 79.73; N, 8.09; H, 7.56. Found: C, 79.70; N, 8.11; H, 7.60.

The ligand of 2-[ethyl(*N*-diisopropylphenylcarboximidate)]quinoline (**L2**). Yield: 62.9%. ^{1}H-NMR (400 MHz, $CDCl_3$, δ, ppm): 7.98 (d, 1H, $H_{quinoline\text{-}4}$), 7.93 (d, 1H, $H_{quinoline\text{-}8}$), 7.71 (d, 1H, $H_{quinoline\text{-}3}$), 7.63 (t, 1H, $H_{quinoline\text{-}5}$), 7.50 (t, 1H, $H_{quinoline\text{-}7}$), 7.32 (d, 1H, $H_{quinoline\text{-}6}$), 6.92–6.98 (m, 3H, H_{Ar}), 4.61 (q, 2H, $-OCH^*_2CH_3$), 3.07 (m, 2H, $-CH^*(CH_3)_2$), 1.53 (t, 3H, $-OCH_2CH^*_3$), 1.15 (d, 6H, $-CH_3$), 0.89 (d, 6H, $-CH_3$). ^{13}C-NMR (100 MHz, $CDCl_3$,

δ, ppm): 154.5, 150.1, 147.3, 143.2, 137.3, 135.9, 130.1, 129.6, 127.5, 127.2, 122.6, 120.2, 62.83, 28.22, 23.6, 22.4, 14.5. FTIR (KBr, cm^{-1}): 3062(w), 2959(m), 2867(m), 1662(s), 1591(m), 1500(m), 1459(m), 1363(m), 1287(m), 1240(m), 1213(m), 1147(m), 1103(m), 1029(m), 919(m), 835(m), 796(m), 759(m), 654(m). Anal. Calcd. for $C_{24}H_{28}N_2O$ (360.2): C, 79.96; N, 7.77; H, 7.83. Found: C, 79.94; N, 7.80; H, 7.86.

The ligand of 2-[phenyl(*N*-diisopropylphenylcarboximidate)]quinoline (**L3**). Yield: 80.2%. ^{1}H-NMR (400 MHz, $CDCl_3$, δ, ppm): 8.15 (d, 1H, $H_{quinoline\text{-}4}$), 7.92 (d, 1H, $H_{quinoline\text{-}8}$), 7.79 (d, 1H, $H_{quinoline\text{-}3}$), 7.65 (t, 1H, $H_{quinoline\text{-}5}$), 7.54 (t, 1H, $H_{quinoline\text{-}7}$), 6.98–7.25 (partially overlapping with $CDCl_3$, $H_{quinoline\text{-}6}$ and H_{Ar}), 3.06 (m, 2H, $-CH^*(CH_3)_2$), 1.12 (s, 12H, $-CH_3$). ^{13}C-NMR (100 MHz, $CDCl_3$, δ, ppm): 154.6, 152.6, 149.7, 147.3, 142.3, 137.1, 136.4, 130.3, 129.8, 129.1, 127.8, 127.3, 124.1, 123.4, 122.7, 121.0, 28.6, 23.2. FTIR (KBr, cm^{-1}): 3067(w), 2964(m), 2862(m), 1673(s), 1586(m), 1483(m), 1458(m), 1433(m), 1375(m), 1316(m), 1243(m), 1210(m), 1125(m), 1078(m), 950(m), 927(m), 862(m), 843(m), 753(m), 692(m). Anal. Calcd. for $C_{28}H_{28}N_2O$ (408.2): C, 82.32; N, 6.86; H, 6.91. Found: C, 82.36; N, 6.90; H, 6.88.

The ligand of 2-[4-chlorophenyl(*N*-diisopropylphenylcarboximidate)]quinoline (**L4**). Yield: 86.1%. ^{1}H-NMR (400 MHz, $CDCl_3$, δ, ppm): 8.16 (d, 1H, $H_{quinoline\text{-}4}$), 7.92 (d, 1H, $H_{quinoline\text{-}8}$), 7.80 (d, 1H, $H_{quinoline\text{-}3}$), 7.67 (t, 1H, $H_{quinoline\text{-}5}$), 7.56 (t, 1H, $H_{quinoline\text{-}7}$), 6.99–7.23 (partially overlapping with $CDCl_3$, $H_{quinoline\text{-}6}$ and H_{Ar}), 3.01 (m, 2H, $-CH^*(CH_3)_2$), 1.10 (s, 12H, $-CH_3$). ^{13}C-NMR (100 MHz, $CDCl_3$, δ, ppm): 153.1, 152.3, 149.1, 147.2, 142.0, 136.9, 136.5, 130.1, 129.9, 129.1, 127.9, 127.3, 123.5, 122.7, 122.2, 120.9, 28.6, 23.1. FTIR (KBr, cm^{-1}): 3077(w), 2959(m), 2867(m), 1674(s), 1593(m), 1488(m), 1431(m), 1381(m), 1319(m), 1211(m), 1121(m), 1070(m), 1011(m), 951(m), 913(m), 848(m), 810(m), 767(m), 727(m). Anal. Calcd. for $C_{28}H_{27}ClN_2O$ (442.2): C, 75.92; N, 6.32; H, 6.14. Found: C, 75.94; N, 6.37; H, 6.15.

*General procedures for the synthesis of ligands **L5**–**L7***

Ligands **L5**–**L7** were prepared in a similar manner. A typical synthetic procedure of ligand **L5** is described as follows:

To a 100 mL flask were added 20 mL of THF and 0.11 g of 1,4-dihydroxybenzene (1 mmol) under nitrogen atmosphere. Then the flask was put into an ice bath and 0.24 g of NaH (10 mmol) was carefully added into the flask (a lot of hydrogen gas bubbled out!). After the mixture was stirred for 30 min at room temperature, 0.7 g of 2-[*N*-(2,6-diisopropylphenyl)carboximidoylchloride]quinoline (2 mmol) in 20 mL of THF was added dropwise into the flask, and the reaction mixture was further refluxed for 12 h. After 10 mL of H_2O and 30 mL of CH_2Cl_2 were carefully added, the mixture was further washed with H_2O (100 mL × 3). The organic layer was collected and dried over anhydrous magnesium sulfate. After evaporating the solvent under reduced pressure, the crude product was purified by silica gel column chromatography (petroleum ether:ethyl acetate, 15:1, *V*:*V*) to afford a yellow solid.

The ligand of **L5**. Yield: 24.9 %. ^{1}H-NMR (400 MHz, $CDCl_3$, δ, ppm): 8.14 (d, 1H, H_e), 7.91 (d, 1H, H_a), 7.80 (d, 1H, H_f), 7.57 (m, 2H, $H_{b,d}$), 7.01–7.11 (m, 6H, $H_{c,g,h,i}$), 3.05 (s, 2H, H_j), 1.09 (s, 12H, H_k). ^{13}C-NMR (100 MHz, $CDCl_3$, δ, ppm): 151.89, 150.10, 148.71, 146.52, 141.60, 136.27, 135.64, 129.57, 129.09, 127.21, 127.13, 126.57, 122.65, 121.94, 120.24, 27.84, 22.50. FTIR (KBr, cm^{-1}): 3058(w), 2957(m), 2924(m), 2866(m), 1693(s), 1593(m), 1499(m), 1462(m), 1379(m), 1283(m), 1236(m), 1187(s), 1132(m), 1094(m), 924(m), 829(m), 771(m), 744(m). Anal. Calcd. for $C_{50}H_{50}N_4O_2$ (738.4): C, 81.27; H, 6.82; N, 7.58. Found: C, 81.36; H, 6.90; N, 7.67. ESI-MS for $C_{50}H_{50}N_4O_2$: (*m*/*z*) (M+H$^+$) 739.4.

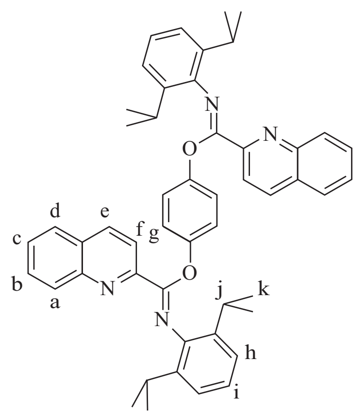

The ligand of **L6**. Yield: 31.7%. ^{1}H-NMR (400 MHz, $CDCl_3$, δ, ppm): 8.16 (d, 1H, H_e), 7.92 (d, 1H, H_a), 7.80 (d, 1H, H_f), 7.66 (t, 1H, H_d), 7.54 (t, 1H, H_b), 6.91–7.05 (m, 8H, $H_{c,\,g,\,h,\,i,\,j}$), 3.04 (m, 2H, H_k), 1.53 (s, 3H, H_m), 1.13 (s, 12H, H_l). FTIR (KBr, cm^{-1}): 3059(w), 2957(m), 2902(m), 2865(m), 1669(s), 1593(m), 1498(s), 1463(m), 1384(m), 1311(m), 1284(m), 1205(s), 1170(m), 1066(m), 1015(m), 909(m), 830(m), 760(m). Anal. Calcd. for $C_{59}H_{60}N_4O_2$ (856.5): C, 82.67; H, 7.06; N, 6.54. Found: C, 82.60; H, 7.03; N, 82.51. ESI-MS for $C_{59}H_{60}N_4O_2$: (*m*/*z*) (M+H$^+$) 857.5.

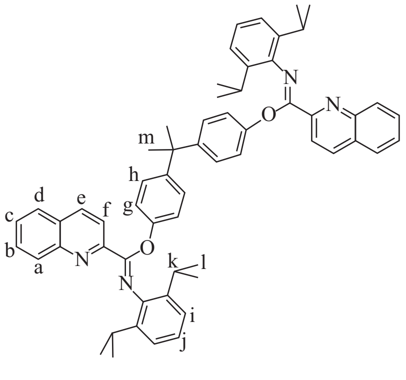

The ligand of **L7**. Yield: 26.4%. ^{1}H-NMR (400 MHz, $CDCl_3$, δ, ppm): 8.15 (d, 1H, H_e), 7.94 (d, 1H, H_a), 7.79 (d, 1H, H_f), 7.66 (t, 1H, H_d), 7.54 (t, 1H, H_b), 6.86–7.04 (m, 8H, $H_{c,\,g,\,h,\,i,\,j}$), 3.82 (s, 1H, H_m), 3.04 (m, 2H, H_k), 1.12 (s, 12H, H_l). FTIR (KBr, cm^{-1}): 3059(w), 2953(m), 2919(m), 2860(m), 1683(s), 1597(m), 1504(s), 1462(m), 1380(m),

https://doi.org/10.1007/s10118-018-2097-8

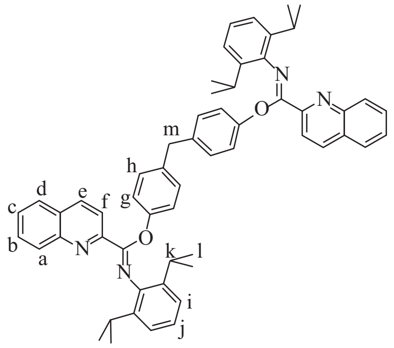

1281(m), 1241(m), 1216(m), 1162(m), 1092(m), 1013(m), 953(m), 911(m), 838(m), 759(m). Anal. Calcd. for $C_{57}H_{56}N_4O_2$ (828.4): C, 82.57; H, 6.81; N, 6.76. Found: C, 82.67; H, 6.90; N, 6.84. ESI-MS for $C_{57}H_{56}N_4O_2$: (*m*/*z*) (M+H$^+$) 829.4.

*General procedures for the synthesis of complexes **Co1**–**Co4***

All the complexes were prepared in a similar method. A typical synthesis procedure of the complex **Co1** is described as follows. A solution of the ligand **L1** (0.17 g, 0.5 mmol) in 2 mL of THF was added dropwise to a suspension of anhydrous $CoBr_2$ (0.11 g, 0.5 mmol) in 2 mL of THF; the reaction mixture was stirred for 10 h. Partial THF was removed under reduced pressure. A large amount of ether (or hexane) was added, as a result, plenty of precipitate was formed. The precipitate was filtered, and dried under vacuum at 40 °C.

The complex of 2-[methyl(*N*-diisopropylphenylcarboximidate)]quinoline $CoBr_2$ (**Co1**). Yield: 74.2%. FTIR (KBr, cm^{-1}): 2959(m), 2872(w), 1622(m), 1586(m), 1506(m), 1462(m), 1440(m), 1386(m), 1326(m), 1260(m), 1222(m), 1124(m), 996(m), 876(m), 845(m), 811(m), 767(m), 643(m). Anal. Calcd. for $C_{23}H_{26}Br_2CoN_2O$ (563.0): C, 48.88; N, 4.96; H, 4.64. Found: C, 48.90; N, 4.91; H, 4.73.

The complex of 2-[ethyl(*N*-diisopropylphenylcarboximidate)]quinoline $CoBr_2$ (**Co2**). Yield: 60.8%. FTIR (KBr, cm^{-1}): 2964(m), 2867(w), 1610(m), 1563(m), 1506(m), 1464(m), 1438(m), 1373(m), 1313(m), 1262(m), 1218(m), 1121(m), 1056(m), 1000(m), 838(m), 796(m), 768(m), 748(m), 641(m). Anal. Calcd. for $C_{24}H_{28}Br_2CoN_2O$ (577.0): C, 49.77; N, 4.84; H, 4.87. Found: 49.81; N, 4.79; H, 4.93.

The complex of 2-[phenyl(*N*-diisopropylphenylcarboximidate)]quinoline $CoBr_2$ (**Co3**). Yield: 74.8%. FTIR (KBr, cm^{-1}): 2964(m), 2867(w), 1627(m), 1581(m), 1503(m), 1490(m), 1465(m), 1386(m), 1322(m), 1261(m), 1218(m), 1201(m), 1166(m), 939(m), 781(m), 764(m), 753(m), 733(m), 688(m). Anal. Calcd. for $C_{28}H_{28}Br_2CoN_2O$ (625.0): C, 53.61; N, 4.47; H, 4.50. Found: C, 53.66; N, 4.51; H, 4.48.

The complex of 2-[4-chlorophenyl(*N*-diisopropylphenylcarboximidate)]quinoline $CoBr_2$ (**Co4**). Yield: 57.7%. FTIR (KBr, cm^{-1}): 2964(m), 2867(w), 1623(m), 1581(m), 1561(m), 1509(m), 1487(m), 1462(m), 1320(m), 1257(m), 1200(m), 1090(m), 1011(m), 830(m), 786(m), 764(m), 667(m). Anal. Calcd. for $C_{28}H_{27}Br_2ClCoN_2O$ (658.9): C, 50.82; N, 4.23; H, 4.11. Found: C, 50.84; N, 4.29; H, 4.09.

The complex of **Co5**. **Co5** was prepared with a similar method as **Co1**–**Co4** by using $CoCl_2$. Yield: 83.2%. FTIR (KBr, cm^{-1}): 3062(w), 2961(m), 2928(m), 2868(m), 1628(m), 1562(m), 1494(m), 1460(m), 1310(m), 1258(m), 1196(m), 1180(m), 1090(w), 928(w), 837(m), 764(m). Anal. Calcd. for $C_{50}H_{50}N_4O_2Co_2Cl_4$ (996.1): C, 60.14; H, 5.05; N, 5.61. Found: C, 60.19; H, 5.11; N, 5.07.

The complex of **Co6**. **Co6** was prepared with a similar method as **Co1**–**Co4** by using $CoCl_2$. Yield: 66.1%. FTIR (KBr, cm^{-1}); 2959(m), 2925(m), 2868(m), 1631(m), 1556(m), 1499(m), 1463(m), 1383(m), 1320(m), 1257(m), 1207(m), 1169(m), 1078(m), 1015(m), 916(m), 834(m), 762(m). Anal. Calcd. For $C_{59}H_{60}Cl_4Co_2N_4O_2$ (1114.2): C, 63.45; H, 5.42; N, 5.02. Found: C, 63.57; H, 5.48; N, 4.97.

The complex of **Co7**. **Co7** was prepared in a similar method as **Co1**–**Co4** by using $CoCl_2$. Yield: 62.8%. FTIR (KBr, cm^{-1}): 2959(m), 2931(m), 2851(m), 1626(m), 1502(m), 1458(m), 1381(m), 1315(m), 1201(m), 1164(m), 1088(m), 1013(m), 923(m), 753(m). Anal. Calcd. For $C_{57}H_{56}Cl_4Co_2N_4O_2$ (1086.1): C, 62.88; H, 5.18; N, 5.15. Found: C, 62.91; H, 5.24; N, 5.26.

General Procedure for the Solution Polymerization of 1,3-Butadiene

A typical procedure for the polymerization is as follows (run 15). A toluene solution of 1,3-butadiene (10 mL, 0.1 g/mL) was added to a moisture free ampule preloaded with complex **Co1** (9.3 μmol), then EASC (0.46 mmol) was injected to initiate the polymerization at 50 °C. After 30 min, ethanol containing 2,6-ditertbutyl-4-methylphenol (1.0 wt%) as a stabilizer was added to quench the polymerization. The precipitated polymer was washed with ethanol, and then dried under vacuum at 40 °C to a constant weight. The yield of polymer was determined by gravimetry.

X-ray Crystallographic Analysis

X-ray analysis for the crystals is described in the experimental section. Data collections were performed at −88.5 °C on a Bruker SMART APEX diffractometer with a CCD area detector, using graphite monochromated Mo K radiation (λ = 0.71073 Å). The determination of crystal class and unit cell parameters was carried out by the SMART program package. The raw frame data were processed using SAINT and SADABS to yield the reflection data file. The structures were solved by using SHELXTL program. Refinement was performed on F^2 anisotropically for all non-hydrogen atoms by the full-matrix least-squares method. The hydrogen atoms were placed at the calculated positions and were included in the structure calculation without further refinement of the parameters. CCDC 1419601 for ligand **L5** and 1037948, 1037949 for complexes **Co1**, **Co3**, and supplementary crystallographic data for this paper can be obtained free of charge from the Cambridge Crystallographic Data Centre through www.ccdc.cam.ac.uk/data_request/cif.

RESULTS AND DISCUSSION

Synthesis and Characterization of the Ligands and Corresponding Co(II) Complexes

A series of quinoline-2-imidate ligands (**L1**–**L7**) were prepared according to the procedures described in Scheme 1

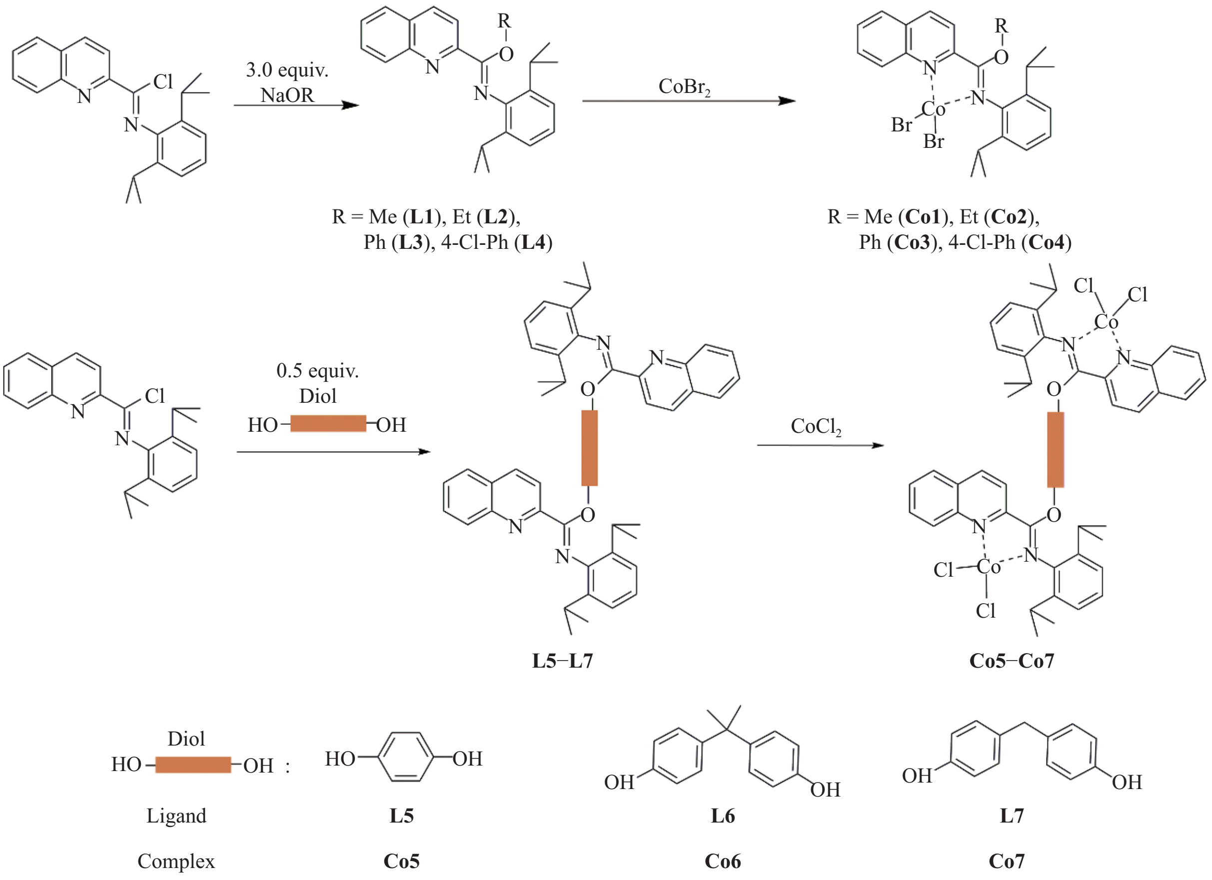

Scheme 1 Synthesis of the ligands (**L1**–**L7**) and Co(II) complexes (**Co1**–**Co7**)

by using the imidoylchloride-based precursors. The corresponding Co(II) complexes were synthesized from the reaction of these ligands with anhydrous $CoBr_2$ or $CoCl_2$ in THF. All of the ligands and complexes were characterized by NMR, IR, and elemental analysis. In the IR spectra, the absorption bands of C=N in complexes **Co1**–**Co7** appear at 1610–1631 cm^{-1}, which are obviously red-shifted as compared to the corresponding ligands (1662–1693 cm^{-1}), indicating that the nitrogen atoms of imidates coordinate to the central metals. The molecular structures of ligand **L5** and complexes **Co1** and **Co3** were further characterized by single-crystal X-ray diffraction, whereas the single crystals of binuclear Co(II) complexes could not be obtained due to their poor solubility. The selected bond distances, bond angles, and crystallographic details of those single crystals are summarized in Tables 1 and 2, and their molecular structures are shown in Figs. 1–4.

Single crystal of ligand **L5** was obtained by recrystallization from its hexane solution, which was suitable for X-ray diffraction analysis. As shown in Fig. 1, it displays centrosymmetric structure with an inversion centre at the 1,4-bisphenol central point. For each half part of the ligand, it exhibits an *E* configuration with O(1) and N(2) atoms placing on the opposite sides of C=N double bond. Similar to the imidoylchloride precursor, the plane formed by N(2)—C(6)—O(1) is not coplanar with quinoline ring and the dihedral is 20.58°, and the 2,6-diisopropylphenyl rings are nearly perpendicular to the quinoline plane with a dihedral angle of 83.83°[43].

Single crystals of **Co1** and **Co3** were grown by layering diethyl ether on a dichloromethane solution of each molecule at room temperature. These complexes adopt isomorphous

Table 1 Selected bond lengths (Å) and angles (°) of ligand **L5** and complexes **Co1** and **Co3**

	L5	Co1	Co3
Bond lengths (Å)			
Co(1)—N(1)	–	2.052 (2)	2.084 (6)
Co(1)—N(2)	–	2.045 (2)	2.040 (5)
C(6)—N(2)	1.254 (3)	1.282 (3)	1.263 (8)
C(6)—O(1)	1.382 (3)	1.321 (3)	1.348 (7)
C(6)—C(5)	1.489 (3)	1.505 (3)	1.493 (10)
Co(1)—Br(1)	–	2.3434 (5)	2.340 (2)
Co(1)—Br(2)	–	2.3596 (4)	2.351 (2)
N(2)—C(7)	1.424 (3)	1.453 (3)	1.481 (9)
Bond angles (°)			
N(1)—Co(1)—N(2)	–	81.64 (8)	80.3 (2)
N(1)—Co(1)—Br(1)	–	112.17 (6)	118.95 (18)
N(1)—Co(1)—Br(2)	–	109.03 (6)	109.81 (17)
Br(1)—Co(1)—Br(2)	–	114.743 (17)	110.20 (6)
Br(1)—Co(1)—N(2)	–	122.00 (6)	116.82 (17)
Br(2)—Co(2)—N(2)	–	112.07 (6)	118.00 (17)
C(5)—C(6)—O(1)	109.37 (19)	110.8 (2)	118.2 (6)
N(2)—C(6)—O(1)	119.3 (2)	130.7 (2)	122.5 (6)
C(5)—C(6)—N(2)	131.3 (2)	118.5 (2)	119.0 (6)
C(6)—N(2)—C(7)	125.5 (2)	124.4 (2)	118.0 (5)

Table 2 Crystallographic data and structure refinement for ligand **L5** and complexes **Co1** and **Co3**

	L5	**Co1**	**Co3**
Formula	$C_{50}H_{50}N_4O_2$	$C_{23}H_{26}Br_2CoN_2O$	$C_{28}H_{28}Br_2CoN_2O$
fw	738.94	565.21	627.27
Color	Yellow	Green	Green
Cryst. Syst.	Monoclinic	Monoclinic	Monoclinic
Space group	P21/c	P21/n	C2/C
a (Å)	8.2434 (8)	10.6652 (7)	20.127 (19)
b (Å)	29.153 (3)	17.1978 (11)	17.035 (16)
c (Å)	9.1705 (9)	12.7099 (8)	17.207 (16)
α (°)	90.0	90	90
β (°)	106.996 (2)	93.496 (1)	114.689 (14)
γ (°)	90.0	90	90
V (Å^3)	2107.6 (4)	2326.9 (3)	5360 (9)
Z	2	4	8
T (K)	185	188	188
D_{calcd} (g·cm^{-3})	1.164	1.613	1.555
μ(Mo Kα) (mm^{-1})	0.07	4.19	3.65
F(000)	788	1132	2520
θ_{range} (°)	2.4–20.1	2.0–25.1	1.6–25.1
No. of rflns collected	11957	13390	27990
No. of indep rflns	3722	4114	4621
data/restraints/params	3722/0/257	4114/0/262	4621/0/307
Goodness of fit	1.039	1.071	1.104
R_1 ($I > 2\sigma(I)$)	0.068	0.027	0.059
wR_2	0.147	0.072	0.191

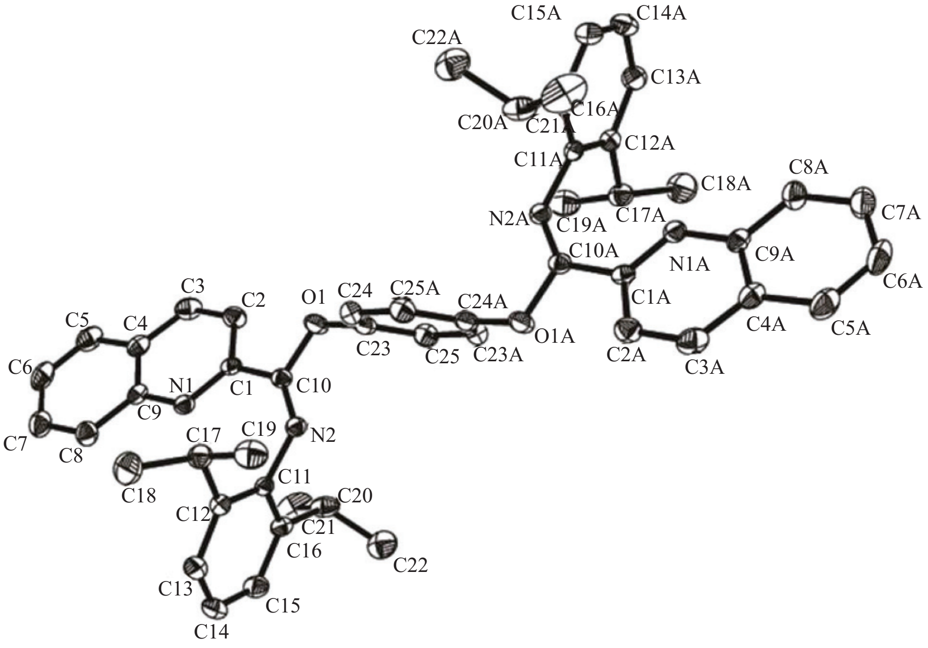

Fig. 1 Molecular structure of ligand **L5** (Hydrogen atoms have been omitted for clarity.)

coordinating geometries around the cobalt center and display distorted tetrahedral structures (see Figs. 2–4). In both complexes, two planes formed by Br(1)—Co(1)—Br(2) and N(1)—Co(1)—N(2) are nearly perpendicular with the dihedral angles of 85.35° and 88.03°, respectively, and the N(1)—Co(1)—N(2) bond angles are relatively small (80.3(2)° and 81.64(8)°). The *N*-bound aryl and quinolinyl rings are also almost perpendicular to each other with the angles of 72.85° for **Co1** and 73.87° for **Co3**, respectively. A similar result was obtained in the previously reported quinoline-2-imino Co(II) complex[50]. In these two complexes, the oxygen atoms on the imidate groups are nearly posited on the plane of quinolinyl rings, from which they deviated by 0.077 and 0.073 Å, respectively.

The Polymerization Behaviors of 1,3-Butadiene in the Presence of Complexes Cobalt(II)

The mono- and binuclear Co(II) complexes were used as precatalysts for the polymerization of 1,3-butadiene. The results are summarized in Tables 3 and 4.

The effects of polymerization parameters, such as the type of cocatalyst and polymerization temperature, were firstly

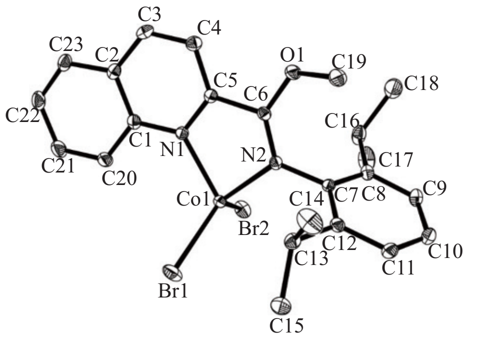

Fig. 2 Molecular structure of complex **Co1** (Hydrogen atoms have been omitted for clarity.)

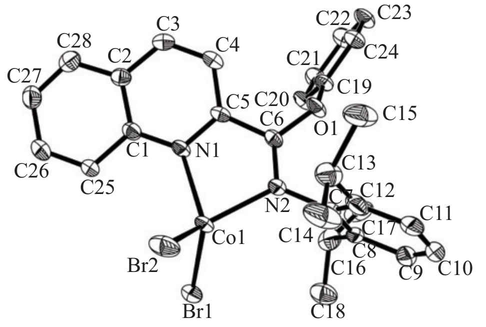

Fig. 3 Molecular structure of complex **Co3** (Hydrogen atoms have been omitted for clarity.)

examined by taking complex **Co1** as an example. According to the data shown in Table 3, in the presence of triethylaluminium (TEA), the complex **Co1** was very inactive. Upon activation with methylaluminoxane (MAO), much better polymer yield (50.8%) was achieved, and the resulting polybutadiene possessed a *cis*-1,4-rich structure (90.5%) and a relatively narrower molecular weight distribution (PDI = 2.3). The systems based on chloroaluminium compounds, diethylaluminium chloride (DEAC) and ethylaluminium sesquichloride (EASC), exhibited high activity, and the polymer yields reached 79.0% and 87.4% within 30 min, respectively. In addition, **Co1**/EASC system also provided polybutadiene with *cis*-1,4-rich structure. Therefore, EASC was used in the following experiments.

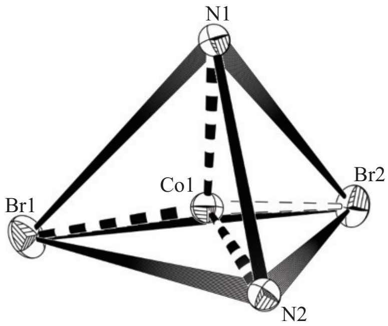

Fig. 4 Coordination geometry of complexes **Co1** (Hydrogen atoms have been omitted for clarity.)

The influence of polymerization temperature on the catalytic performance was further investigated with **Co1**/EASC system. The activity increased with the temperature increased from 0 °C to 50 °C, whereas a further increase in the polymerization temperature resulted in a decrease of activity. These results indicate that the present **Co1**/EASC system suffers from the decay of catalytic activity at high temperature due to the instability of the active species at elevated temperatures. This is similar to the most previously reported late transition metal catalyst[25, 51]. On the other hand, when the polymerization temperature increased from 0 °C to 70 °C, the molecular weight of resulting polybutadienes decreased from 5.81×10^4 to 0.90×10^4 and the molecular weight distribution became broad, indicating that the chain transfer reactions was facilitated at high temperatures. Meanwhile, the *cis*-1,4- content decreased from 97.1% to 78.7% along with the *trans*-1,4- and 1,2- content increasing from 2.1% and 0.8% to 7.8% and 5.0%, respectively. Similar phenomena were also observed in the other Co(II) systems. It is attributable to the facilitation of *anti-syn* isomerization through *π-σ* rearrangement at elevated temperatures[28, 37, 42].

The influence of substituent at imidate-carbon position on catalytic behavior was further investigated. The results are listed in Table 4. For the mononuclear cobalt complexes, changing the steric bulkiness of alkyl ether group from MeO—, EtO— to PhO— showed almost no influence on catalytic performance, which might be due to the long distance between these alkyl ethers and the active species. On the other hand, introducing an electron-withdrawing chlorine atom to the phenylether ring made the catalytic precursor more active (**Co4** versus **Co3**), which is possibly owing to the enhanced electropositivity with the cobalt

Table 3 1,3-Butadiene polymerization with **Co1** under different conditions

Run [a]	Cat.	Polymerization conditions		Yield (%)	M_n [d] × 10^{-4}	M_w/M_n [d]	Microstructure [e] (%)		
		Al [c]	T (°C)				*Cis*-1,4	*Trans*-1,4	1,2-
1	**Co1**	EASC	0	19.7	5.81	2.1	97.1	2.1	0.8
2	**Co1**	EASC	20	61.4	5.40	2.1	96.8	2.0	1.2
3	**Co1**	EASC	50	87.4	3.31	4.5	89.7	7.8	2.5
4	**Co1**	EASC	70	82.0	0.90	5.8	78.7	16.3	5.0
5	**Co1**	MAO [b]	50	50.8	2.19	2.3	90.5	5.9	3.6
6	**Co1**	TEA [b]	50	No polymer	–	–	–	–	–
7	**Co1**	DEAC [b]	50	79.0	0.76	3.3	71.1	11.0	17.9

[a] Polymerization conditions: [Bd]/[Co] = 2000, [Al]/[Co] = 50, [Bd] = 0.1 g/mL, toluene, 10 mL, 30 min. [b] Polymerization time 4 h; [c] EASC: ethylaluminium sesquichloride, MAO: methylaluminoxane, TEA: triethylaluminium, DEAC: diethylaluminium chloride; [d] Determined by GPC eluted with THF (polystyrenes as standards); [e] Determined by IR and NMR

Table 4 1,3-Butadiene polymerization with Co(II) complexes bearing different ligand environments

Run [a]	Cat.	*T* (°C)	Yield (%)	$M_n \times 10^{-4}$	M_w/M_n	Microstructure (%)		
						Cis-1,4	*Trans*-1,4	1,2-
8	**Co1**	50	87.4	3.31	4.5	89.7	7.8	2.5
9	**Co2**	50	86.0	2.93	3.1	90.6	6.8	2.6
10	**Co3**	50	88.0	2.73	3.0	91.1	6.7	2.2
11	**Co4**	50	91.6	3.32	3.1	90.9	6.6	2.5
12	**Co5**	0	19.5	56.1	1.6	98.2	1.1	0.7
13	**Co5**	20	51.2	20.6	2.9	98.1	0.9	1.0
14	**Co5**	50	94.3	5.1	11.5	89.8	3.0	7.2
15	**Co5**	70	95.5	3.7	11.5	79.6	15.4	5.0
16	**Co6**	0	17.5	36.1	1.9	98.0	0.9	1.1
17	**Co6**	20	50.6	33.2	2.1	97.9	1.2	0.9
18	**Co6**	50	95.6	6.7	7.3	91.8	5.7	2.5
19	**Co6**	70	94.3	3.6	15.4	82.6	13.2	4.2
20	**Co7**	0	16.6	26.3	1.9	98.4	0.7	0.9
21	**Co7**	20	58.0	24.3	2.3	97.9	1.0	1.1
22	**Co7**	50	95.3	8.5	5.7	91.1	6.2	2.7
23	**Co7**	70	97.2	4.2	9.2	83.5	12.4	4.1

[a] Polymerization conditions: [Bd]/[Co] = 2000, EASC, [Al]/[Co] = 50, [Bd] = 0.1 g/mL, toluene, 10 mL, 30min

centre. Compared with the mononuclear complexes, their binuclear counterparts displayed higher catalytic activity under identical conditions probably due to the high local precatalyst concentrations. Similar results were observed in the cases of binuclear titanium catalytsts for ethylene polymerization, in which the binuclear precursors also displayed much higher catalytic activity[44].

As previously reported, most of the late-transition metal systems suffered from severe decay of catalytic activity when exposed to high temperature. For the present binuclear Co(II) complexes, their ligands were relatively rigid due to the biphenol linker, and thus we examined their thermal responses under different temperatures. As shown by runs 12–23 in Table 4, for all of the binuclear Co(II) compounds, their catalytic activity dramatically increased when the temperature increased from 0 °C to 50 °C. Further increasing the temperature to 70 °C, no obvious decrease of activity was observed, indicating that these binuclear complexes displayed much higher thermal stability compared to their mono- counterparts, which revealed that rigidifying the ligand could partially increase the thermal stability of the corresponding complexes. Despite of these results, resembling to other Co(II) systems, the molecular weight of the resulting polymers dropped seriously from 56.1×10^4 (**Co5**), 36.1×10^4 (**Co6**), 26.3×10^4 (**Co7**) to 3.7×10^4 (**Co5**), 3.6×10^4 (**Co6**), 4.2×10^4 (**Co7**), respectively, due to the facilitated chain transfer reaction. Besides, the *cis*-1,4- content of the resulting polymer also decreased from 98.2% (**Co5**), 98.0% (**Co6**), 98.4% (**Co7**) to 79.6% (**Co5**), 82.6% (**Co6**), 83.5% (**Co7**) respectively, caused by the *anti-syn* isomerization at high temperatures[28, 37, 42].

CONCLUSIONS

Mono- and binuclear Co(II) complexes were synthesized, and their catalytic activity towards 1,3-butadiene polymerization was investigated. Using EASC as the cocatalyst, all of the complexes performed high activity and high *cis*-1,4- selectivity at 50 °C. For mononuclear Co(II) complexes, increasing the temperature resulted in the negative effects, in contrast, the binuclear Co(II) counterparts performed high temperature tolerance, displaying high activity even at high temperatures. For both mono- and binuclear systems, increasing the temperature brought monotonous reduction of *cis*-1,4- moiety and increment of *trans*-1,4- moiety.

ACKNOWLEDGMENTS

This work was financially supported by the National Key R&D Program of China (No. 2017YFB0307100 (2017YFB0307103)) and National Basic Research Program of China (No. 2015CB654700 (2015CB654702)).

REFERENCES

1 Johnson, L. K.; Killian, C. M.; Brookhart, M. New Pd(II)-based and Ni(II)-based catalysts for polymerization of ethylene and alpha-olefins. J. Am. Chem. Soc. 1995, 117(23), 6414−6415.

2 Johnson, L. K.; Mecking, S.; Brookhart, M. Copolymerization of ethylene and propylene with functionalized vinyl monomers by palladium(II) catalysts. J. Am. Chem. Soc. 1996, 118(1), 267−268.

3 Ittel, S. D.; Johnson, L. K.; Brookhart, M. Late-metal catalysts for ethylene homo- and copolymerization. Chem. Rev. 2000, 100(4), 1169−1204.

4 Ma, J.; Feng, C.; Wang, S.; Zhao, K.Q.; Sun, W.H.; Redshaw, C.; Solan, G. A. Bi- and tri-dentate imino-based iron and cobalt pre-catalysts for ethylene oligo-/polymerization. Inorg. Chem. Front. 2014, 1(1), 14−34.

5 Gibson, V. C.; Redshaw, C.; Solan, G. A. Bis(imino)pyridines: Surprisingly reactive ligands and a gateway to new families of catalysts. Chem. Rev. 2007, 107(5), 1745−1776.

6 Britovsek, G. J. P.; Bruce, M.; Gibson, V. C.; Kimberley, B. S.; Maddox, P. J.; Mastroianni, S.; McTavish, S. J.; Redshaw, C.; Solan, G. A.; Stromberg, S.; White, A. J. P.; Williams, D. J. Iron and cobalt ethylene polymerization catalysts bearing 2,6-bis(imino)pyridyl ligands: Synthesis, structures, and polymerization studies. J. Am. Chem. Soc. 1999, 121(38), 8728−8740.

7 Rose, J. Living polymerization of α-olefins with an α-diimine Ni(II) catalyst: formation of well-defined ethylene-propylene copolymers through controlled chain-walking. J. Am. Chem. Soc. 2006, 128(13), 4186−4187.

8 Yu, J.; Liu, H.; Zhang, W.; Hao, X.; Sun, W.H. Access to highly active and thermally stable iron procatalysts using bulky 2-[1-(2,6-dibenzhydryl-4-methylphenylimino)ethyl]-6-[1-(arylimino)ethyl]pyridine ligands. Chem. Commun. 2011, 47(11), 3257−3259.
9 Makio, H.; Terao, H.; Iwashita, A.; Fujita, T. FI catalysts for olefin polymerization—a comprehensive treatment. Chem. Rev. 2011, 111(3), 2363−2449.
10 Wu, J.; Li, Y. Well-defined vanadium complexes as the catalysts for olefin polymerization. Coord. Chem. Rev. 2011, 255(19-20), 2303−2314.
11 Yue, E.; Zhang, L.; Xing, Q.; Cao, X. P.; Hao, X.; Redshaw, C.; Sun, W. H. 2-(1-(2-Benzhydrylnaphthylimino)ethyl) pyridylnickel halides: synthesis, characterization, and ethylene polymerization behavior. Dalton Trans. 2014, 43(2), 423−431.
12 Pan, H.; Zhu, L.; Li, J.; Zang, D.; Fu, Z.; Fan, Z. A thermal stable *α*-diimine palladium catalyst for copolymerization of ethylene with functionalized olefins. J. Mol. Cat. A: Chem. 2014, 390, 76−82.
13 Dai, S.; Sui, X.; Chen, C. Synthesis of high molecular weight polyethylene using iminopyridyl nickel catalysts. Chem. Commun. 2016, 52(58), 9113−9116.
14 Liu, J.; Chen, D.; Wu, H.; Xiao, Z.; Gao, H.; Zhu, F.; Wu, Q. Polymerization of *α*-olefins using a camphyl *α*-diimine Nickel catalyst at elevated temperature. Macromolecules 2014, 47(10), 3325−3331.
15 Song, K.; Yang, W.; Li, B.; Liu, Q.; Redshaw, C.; Li, Y.; Sun, W. H. Nickel(ii) complexes bearing 4,5-bis(arylimino)pyrenylidenes: synthesis, characterization, and ethylene polymerization behaviour. Dalton Trans. 2013, 42(25), 9166−9175.
16 Mu, H.; Pan, L.; Song, D.; Li, Y. Neutral nickel catalysts for olefin homo- and copolymerization: relationships between catalyst structures and catalytic properties. Chem. Rev. 2015, 115(22), 12091−12137.
17 Du, S.; Kong, S.; Shi, Q.; Mao, J.; Guo, C.; Yi, J.; Liang, T.; Sun, W. H. Enhancing the activity and thermal stability of nickel complex precatalysts using 1-[2,6-bis(bis(4-fluorophenyl)methyl)-4-methyl phenylimino]-2-arylimino acenaphthylene derivatives. Organometallics 2015, 34(3), 582−590.
18 Suo, H.; Zhao, T.; Wang, Y.; Ban, Q.; Sun, W. H. *N*-(2,2-dimethyl-1-(quinolin-2-yl)propylidene) arylaminonickel complexes and their ethylene oligomerization. Molecules 2017, 22(4), 630.
19 Gong, D.; Wang, B.; Bai, C.; Bi, J.; Wang, F.; Dong, W.; Zhang, X.; Jiang, L. Metal dependent control of *cis*-/*trans*-1,4 regioselectivity in 1,3-butadiene polymerization catalyzed by transition metal complexes supported by 2,6-bis[1-(iminophenyl)ethyl]pyridine. Polymer 2009, 50(26), 6259−6264.
20 Chen, H. Controlled polymerization of isoprene promoted by a type of hemilabile X[double bond, length as m-dash]PN3 (X = O, S) ligand supported cobalt(ii) complexes: the role of a hemilabile donor on the level of control. Polym. Chem. 2017, 8(11), 1805−1814.
21 Jiang, X.; Wen, X.; Sun, W. H.; He, A. Polymerization of isoprene catalyzed by 2-(methyl-2-benzimidazolyl)-6-(1-(arylimino) ethyl) pyridine iron(III) trichloride with an additional donor. J. Polym. Sci., Part A: Polym. Chem. 2014, 52(17), 2398−2398.
22 Liu, H.; Yang, S. Z.; Wang, F.; Bai, C. X.; Hu, Y. M; Zhang, X. Q. Polymerization of 1,3-butadiene catalyzed by cobalt(II) and nickel(II) complexes bearing pyridine-2-imidate ligands. Chinese J. Polym. Sci. 2016, 34(9), 1060−1069.
23 Gong, D.; Jia, X.; Wang, B.; Wang, F.; Zhang, C.; Zhang, X.; Jiang, L.; Dong, W. Highly *trans*-1,4 selective polymerization of 1,3-butadiene initiated by iron(III) bis(imino)pyridyl complexes. Inorg. Chim. Acta 2011, 373(1), 47−53.
24 Wang, B.; Bi, J.; Zhang, C.; Dai, Q.; Bai, C.; Zhang, X.; Hu, Y.; Jiang, L. Highly active and *trans*-1,4 specific polymerization of 1,3-butadiene catalyzed by 2-pyrazolyl substituted 1,10-phenanthroline ligated iron(II) complexes. Polymer 2013, 54(19), 5174−5181.
25 Ai, P.; Chen, L.; Guo, Y.; Jie, S.; Li, B. G. Polymerization of 1,3-butadiene catalyzed by cobalt(II) and nickel(II) complexes bearing imino- or amino-pyridyl alcohol ligands in combination with ethylaluminum sesquichloride. J. Organom. Chem. 2012, 705(0), 51−58.
26 Cariou, R.; Chirinos, J. J.; Gibson, V. C.; Jacobsen, G.; Tomov, A. K.; Britovsek, G. J. P.; White, A. J. P. The effect of the central donor in bis(benzimidazole)-based cobalt catalysts for the selective *cis*-1,4-polymerisation of butadiene. Dalton Trans. 2010, 39(38), 9039−9045.
27 Gong, D.; Wang, B.; Jia, X.; Zhang, X. The enhanced catalytic performance of cobalt catalysts towards butadiene polymerization by introducing a labile donor in a salen ligand. Dalton Trans. 2014, 43(10), 4169−4178.
28 Jie, S.; Ai, P.; Li, B. Highly active and stereospecific polymerization of 1,3-butadiene catalyzed by dinuclear cobalt(II) complexes bearing 3-aryliminomethyl-2-hydroxybenzaldehydes. Dalton Trans. 2011, 40(41), 10975−10982.
29 Endo, K.; Hatakeyama, N. Stereospecific and molecular weight-controlled polymerization of 1,3-butadiene with Co(acac)3-MAO catalyst. J. Polym. Sci., Part A: Polym. Chem. 2001, 39(16), 2793−2798.
30 Gong, D.; Wang, B.; Cai, H.; Zhang, X.; Jiang, L. Synthesis, characterization and butadiene polymerization studies of cobalt(II) complexes bearing bisiminopyridine ligand. J. Organom. Chem. 2011, 696(8), 1584−1590.
31 Jia, X.; Liu, H.; Hu, Y.; Dai, Q.; Bi, J.; Bai, C.; Zhang, X. Highly active and *cis*-1,4 selective polymerization of 1,3-butadiene catalyzed by cobalt(II) complexes bearing *α*-diimine ligands. Chin. J. Cat. 2013, 34(8), 1560−1569.
32 Alnajrani, M. N.; Mair, F. S. Synthesis and characterization of [small beta]-triketimine cobalt complexes and their behaviour in the polymerization of 1,3-butadiene. Dalton Trans. 2014, 43(42), 15727−15736.
33 Alnajrani, M. N.; Mair, F. S. The behaviour of [small beta]-triketimine cobalt complexes in the polymerization of isoprene. RSC Adv. 2015, 5(57), 46372−46385.
34 Chandran, D.; Kwak, C. H.; Ha, C. S.; Kim, I. Polymerization of 1,3-butadiene by bis(salicylaldiminate)cobalt(II) catalysts combined with organoaluminium cocatalysts. Catal. Today 2008, 131(1-4), 505−512.
35 Endo, K.; Kitagawa, T.; Nakatani, K. Effect of an alkyl substituted in salen ligands on 1,4-cis selectivity and molecular weight control in the polymerization of 1,3-butadiene with (salen)Co(II) complexes in combination with methylaluminoxane. J. Polym. Sci., Part A: Polym. Chem. 2006, 44(13), 4088−4094.
36 Guo, J.; Zhang, C.; Bi, J.; Zhang, H.; Bai, C.; Hu, Y.; Zhang, X. Cobalt complexes bearing pyridine-imino ligands with bulky aryl substituents: synthesis, characterization, and 1,3-butadiene polymerization behaviors. J. Organom. Chem. 2015, 798, 414−421.
37 Wang, B.; Gong, D.; Bi, J.; Dai, Q.; Zhang, C.; Hu, Y.; Zhang, X.; Jiang, L. Synthesis, characterization and 1,3-butadiene polymerization behaviors of cobalt complexes bearing 2-pyrazolyl-substituted 1,10-phenanthroline ligands. Appl. Organomet. Chem. 2013, 27(4), 245−252.
38 Guo, J.; Wang, B.; Bi, J.; Zhang, C.; Zhang, H.; Bai, C.; Hu, Y.; Zhang, X. Synthesis, characterization and 1,3-butadiene polymerization studies of cobalt dichloride complexes bearing pyridine bisoxazoline ligands. Polymer 2015, 59(24), 124−132.

39 Appukuttan, V.; Zhang, L.; Ha, J. Y.; Chandran, D.; Bahuleyan, B. K.; Ha, C.S.; Kim, I. Stereospecific polymerizations of 1,3-butadiene catalyzed by Co(II) complexes ligated by 2,6-bis(benzimidazolyl)pyridines. J. Mol. Catal. A: Chem. 2010, 325(1-2), 84−90.

40 Gong, D.; Jia, X.; Wang, B.; Zhang, X.; Jiang, L. Synthesis, characterization, and butadiene polymerization of iron(III), iron(II) and cobalt(II) chlorides bearing 2,6-bis(2-benzimidazolyl)pyridyl or 2,6-bis(pyrazol)pyridine ligand. J. Organom. Chem. 2012, 702(1), 10−18.

41 Appukuttan, V.; Zhang, L.; Ha, C. S.; Kim, I. Highly active and stereospecific polymerizations of 1,3-butadiene by using bis(benzimidazolyl)amine ligands derived Co(II) complexes in combination with ethylaluminum sesquichloride. Polymer 2009, 50(5), 1150−1158.

42 Liu, H.; Jia, X.; Wang, F.; Dai, Q.; Wang, B.; Bi, J.; Zhang, C.; Zhao, L.; Bai, C.; Hu, Y.; Zhang, X. Synthesis of bis(*N*-arylcarboximidoylchloride)pyridine cobalt(ii) complexes and their catalytic behavior for 1,3-butadiene polymerization. Dalton Trans. 2013, 42(37), 13723−13732.

43 Liu, H.; Wang, F.; Jia, X.; Liu, L.; Bi, J.; Zhang, C.; Zhao, L.; Bai, C.; Hu, Y.; Zhang, X. Synthesis, characterization, and 1,3-butadiene polymerization studies of Co(II), Ni(II), and Fe(II) complexes bearing 2-(*N*-arylcarboximidoylchloride)quinoline ligand. J. Mol. Cat. A: Chem. 2014, 391, 25−35.

44 Delferro, M.; Marks, T. J. Multinuclear Olefin Polymerization Catalysts. Chem. Rev. 2011, 111(2), 2450−2485.

45 Sun, W.H.; Xing, Q.; Yu, J.; Novikova, E.; Zhao, W.; Tang, X.; Liang, T.; Redshaw, C. Probing the characteristics of mono- or bimetallic (iron or cobalt) complexes bearing 2,4-bis(6-iminopyridin-2-yl)-3H-benzazepines:synthesis,characterization, and ethylene reactivity. Organometallics 2013, 32(8), 2309−2318.

46 Han, S.; Yao, E.; Qin, W.; Zhang, S.; Ma, Y. Binuclear heteroligated titanium catalyst based on phenoxyimine ligands: synthesis, characterization, and ethylene (Co)polymerization. Macromolecules 2012, 45(10), 4054−4059.

47 Salata, M. R.; Marks, T. J. Synthesis, characterization, and marked polymerization selectivity characteristics of binuclear phenoxyiminato organozirconium catalysts. J. Am. Chem. Soc. 2008, 130(1), 12−13.

48 Wang, R.; Sui, X.; Pang, W.; Chen, C. Ethylene polymerization by xanthene-bridged dinuclear α-diimine NiII complexes. Chemcatchem 2016, 8(2), 434−440.

49 Liu, J.; Li, Y.; Liu, J.; Li, Z. Ethylene polymerization with a highly active and long-lifetime macrocycle trinuclear 2,6-bis(imino)pyridyliron. Macromolecules 2005, 38(7), 2559−2563.

50 Song, S.; Zhao, W.; Wang, L.; Redshaw, C.; Wang, F.; Sun, W. Synthesis, characterization and catalytic behavior toward ethylene of cobalt(II) and iron(II) complexes bearing 2-(1-aryliminoethylidene)quinolines. J. Organom. Chem. 2011, 696(18), 3029−3035.

51 Liu, H.; Wang, F.; Liu, L.; Dong, B.; Zhang, H.; Bai, C.; Hu, Y.; Zhang, X. Synthesis, characterization and 1,3-butadiene polymerization behaviors of three ONO, ONN, and NNN tridentate Co(II) complexes. Inorg. Chim. Acta 2014, 421, 284−291.